

## Article

# Spatial-Temporal Dynamic Evaluation of Ecosystem Service Value and Its Driving Mechanisms in China

Xiaojian Wei <sup>1,2</sup> , Li Zhao <sup>1,\*</sup>, Penggen Cheng <sup>1,2</sup>, Mingrui Xie <sup>1</sup> and Huimin Wang <sup>3</sup>

<sup>1</sup> School of Geomatics, East China University of Technology, 418 Guanglan Road, Nanchang 330013, China; weixiaojian1988@ecut.edu.cn (X.W.); 198560017@ecut.edu.cn (P.C.); 2021110457@ecut.edu.cn (M.X.)

<sup>2</sup> Key Laboratory of Mine Environmental Monitoring and Improving around Poyang Lake, Ministry of Natural Resources, 418 Guang-Lan Road, Nanchang 330013, China

<sup>3</sup> College of Urban and Rural Construction, Zhongkai University of Agriculture and Engineering, Guangzhou 510225, China; wanghuimin@zhku.edu.cn

\* Correspondence: 2020110382@ecut.edu.cn; Tel.: +86-157-7920-4876

**Abstract:** Understanding the spatial differentiation and driving mechanisms of ecosystem service value (ESV) is helpful for the protection and sustainable development of the ecological environment. Despite the fact that various studies on ESV have been conducted in various regions, few studies have discussed the spatial differentiation characteristics of ESV in a long time series at a national scale, and even fewer studies have thoroughly examined the driving mechanism of the spatial differentiation of ESV from the perspective of different regions. On the basis of China's land use data from 1990 to 2018, this paper used the methods of land use dynamics, the ESV evaluation model, hot spot analysis, the barycenter model, and the geographical detector model to study the temporal and spatial differentiation characteristics of land use and ESV in the study area. Moreover, it analyzes the driving mechanisms of the spatial differentiation of ESV at the national scale and in different regions of China. Our results showed the following: (1) Other land types have increased overall, with the exception of grassland. Obvious differences were observed in the single land use dynamics of each land type, especially the construction land, where farmland was the primary source of construction land. With the passage of time, the dynamic degree of comprehensive land use increased. (2) During the study period, ESV generally showed a decreasing trend, with distinct characteristics in high and low ESV areas. The center of gravity of ESV was constantly in Dingxi County and Pingliang City, Shaanxi Province, and its trajectory was generally "S"-shaped. (3) From the perspective of national scale and different regions, the dominant factors affecting the spatial differentiation of ESV were different, and the interaction among multiple factors was significantly stronger than that of a single factor. The findings of the study can provide more scientific decision-making services for China in order to promote regional environmental protection and develop ecological civilization.

**Keywords:** land use; the evaluation model of ecosystem service value; geographical detector model; spatial heterogeneity



**Citation:** Wei, X.; Zhao, L.; Cheng, P.; Xie, M.; Wang, H. Spatial-Temporal Dynamic Evaluation of Ecosystem Service Value and Its Driving Mechanisms in China. *Land* **2022**, *11*, 1000. <https://doi.org/10.3390/land11071000>

Academic Editors: Clara Garcia-Mayor and Almudena Nolasco-Cirugeda

Received: 28 May 2022

Accepted: 28 June 2022

Published: 30 June 2022

**Publisher's Note:** MDPI stays neutral with regard to jurisdictional claims in published maps and institutional affiliations.



**Copyright:** © 2022 by the authors. Licensee MDPI, Basel, Switzerland. This article is an open access article distributed under the terms and conditions of the Creative Commons Attribution (CC BY) license (<https://creativecommons.org/licenses/by/4.0/>).

## 1. Introduction

Ecosystem services (ES) refer to the life-supporting products and services provided to human beings directly or indirectly by ecosystems under good ecological conditions [1,2]. Ecosystem service value (ESV) is an effective quantitative assessment method which highlights the importance of natural assets for human welfare and translates ecological services into practical applications [3,4]. Numerous factors, including natural and social factors, influence the spatial pattern and evolution of ESV. We can reflect the state of the ecosystem in a deeper level by studying changes in the external spatial pattern and internal influence mechanism of ESV, which is highly important for regional planning and effective protection of the ecosystem [5].

Since Costanza (1997) [6] first proposed the concept of ESV, the related research on ESV has always been the major focus in geography and ecology [7,8]. At present, ESV can be assessed in three ways: by the monetary, physical, and energy forms. The monetary assessment method is the easiest and most widely used [9]. It can increase public awareness of the importance of ecosystem services in social development [10]. Scholars have primarily used the ESV equivalent factor table made by Costanza (1997) [6] and Xie (2008) [11] to calculate the ESV of different ecosystems in recent years. However, the monetary assessment is based on a subjective value coefficient that ignores the social development of various regions in different times, resulting in some limitations of this evaluation method. As a result, ESV should be revised in this study to produce more accurate ESV that is more in accordance with the actual situation [9,12].

At present, studies on ESV have gradually changed from evaluation to analysis of ESV's temporal and spatial changes and driving mechanism [13]. For the analysis of temporal and spatial differentiation of ESV, previous studies have focused on farmland [14], wetlands [15], and lakes [16]. For the driving mechanism of changes in ESV, the driving factors mainly include natural and socioeconomic factors [17,18]. The commonly used methods are spatial autocorrelation analysis, logistic regression, and grey correlation degree [19,20], most of which ignore the spatial correlation between the driving factors and fail to reflect the internal complex coupling effect. The geographical detector model (GDM) is an effective tool for exploring the relationship between geographical phenomena and driving factors, and it can help understand ESV's spatial heterogeneity and multifactor interaction mechanism [21,22]. For the research scales of the temporal and spatial changes and the driving mechanism of ESV, the majority of research objects are concentrated in provinces [23], cities [24], urban agglomeration [25], and other local areas. However, little relevant research has been conducted at the macro scale, especially at the national scale. At the same time, in view of the large span of the macro scale from north to south and east to west, the primary factors that influence the spatial and temporal differentiation of ESV in different regions are varied. Currently, only a few studies have been conducted on the evolution of the driving mechanism of the spatiotemporal differentiation of ESV from the perspective of different regions.

Therefore, to better understand the temporal and spatial differentiation characteristics and driving mechanism of China's ESV, this study uses the dynamic degree of land use and the calculation model of ESV to calculate the quantitative changes in land use and ESV. Moreover, it analyzes the spatial change in ESV with the help of hot spot analysis and the barycenter model. Finally, it uses GDM to analyze the driving mechanism of influencing factors on ESV. Specifically, this study aims to: (1) evaluate the temporal and spatial distribution characteristics of land use and ESV in China from 1990 to 2018; and (2) determine the driving forces leading to the spatial differentiation of ESV and their effects. Our study provides a new perspective on the driving mechanism of ecosystem service function, and the results can provide scientific guidance for the optimization of ecosystem protection and management.

## 2. Materials and Methods

### 2.1. Data Sources and Preparation

The land use data for 1990, 2000, 2010, and 2018 in China were derived from the Data Center for Resources and Environmental Sciences of the Chinese Academy of Sciences (1 km resolution). Land use was divided into six types: farmland, woodland, grassland, water body, construction land, and unused land (Figure 1). The socioeconomic data (grain price and the relevant calculation indexes of Engel coefficient) for the corresponding years were from the China Statistical Yearbook and the China Urban Statistical Yearbook. Except for Hong Kong, Macau, and Taiwan, the study focused on prefecture-level and above urban units in China, including prefecture-level and above cities and provincial county-level administrative units. In addition, some socioeconomic data in Zhenjiang, Huaiyin, and Suqian Cities were lacking, and the 1990 Urban Statistical Yearbook in

Xinjiang Uygur Autonomous Region was missing, making some data impossible to collect. To interpolate these data, we used data from adjacent years' statistics yearbooks and data from surrounding cities and counties in the same province.

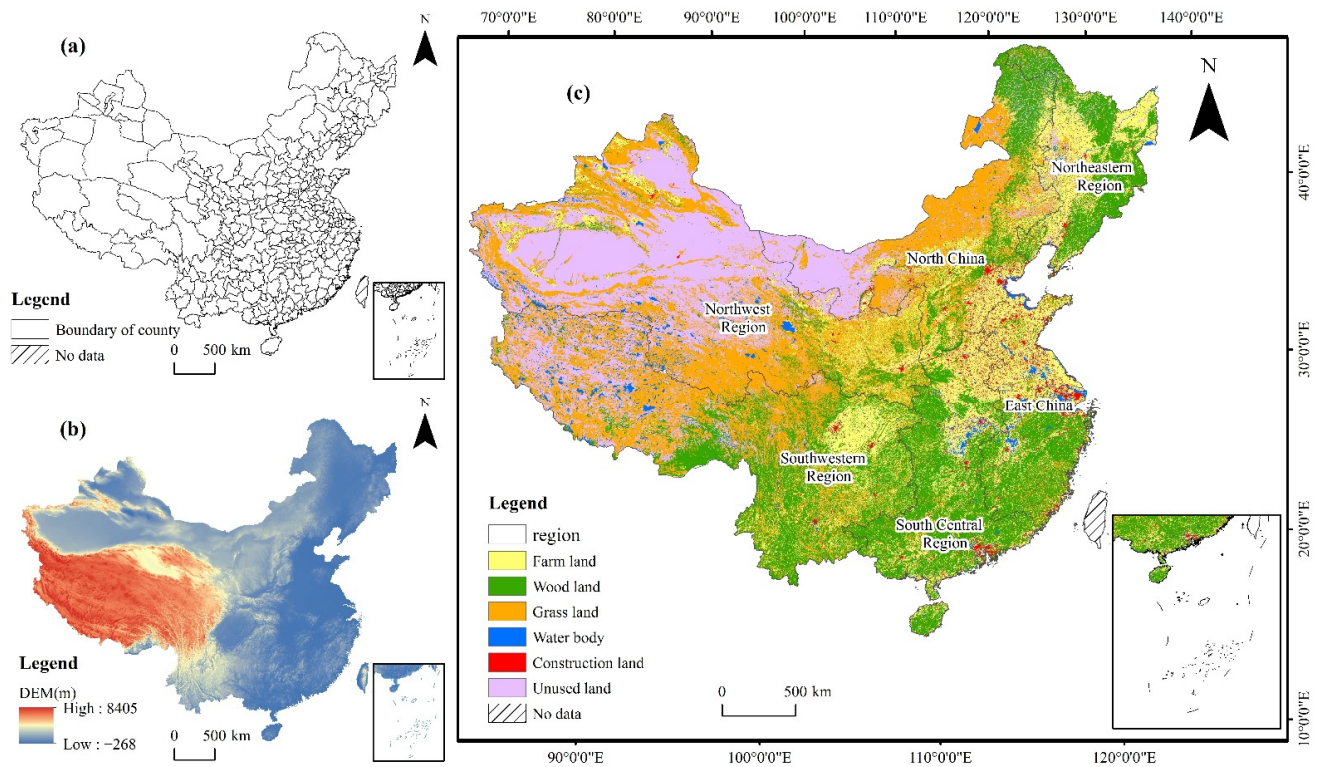


**Figure 1.** Map of the study area ((a): prefecture-level and above cities of China, (b): DEM of China, (c): LUC and six regions of China).

To explore the socioeconomic and natural factors driving the change of ESV, we selected nine driving factors, namely, slope, elevation, temperature, precipitation, normalized difference vegetation index (NDVI) [26], population density, gross domestic product (GDP), construction land intensity, and distance from road. Due to the lack of data on some driving factors, this paper only studied the driving mechanism of the temporal and spatial differentiations of ESV in 2000 and 2018. The digital elevation model (DEM) [27] and NDVI data were obtained from the Data Center for Resources and Environmental Sciences of the Chinese Academy of Sciences (<http://www.resdc.cn>, accessed on 1 January 2022). DEM data could be used to extract slope and elevation distribution characteristics within the study area. Meteorological data were acquired from the National Geospatial Data Cloud platform of China (<http://www.geodata.cn/data/>, accessed on 1 January 2022), which could reflect the regional changes in precipitation and temperature. The population data were obtained from the World Pop Data Center. GDP was obtained from the China Urban Statistical Yearbook. Construction land intensity was calculated with land use data. Road data were provided by OpenStreetMap (which accessed on 1 January 2022, <http://www.openstreetmap.org/>).

## 2.2. Methods

### 2.2.1. Land Use Dynamic Degree

Land use dynamic degree is an important index for analyzing the change dynamics of land use, including single and comprehensive dynamic degrees [9,28].

(1) Single dynamic degree ( $K$ ). Single dynamic degree refers to the change of a certain land use type in a certain period. The calculation formula is as follows:

$$K = \frac{(U_b - U_a)}{U_a} \times \frac{1}{T} \times 100\% \quad (1)$$

where  $U_a$  and  $U_b$  refer to the areas of the specific land use type at the start date and end date ( $\text{km}^2$ ), respectively; and  $T$  is the study period.

(2) Comprehensive dynamic degree ( $LC$ ). Comprehensive dynamic degree refers to the change rate of all land use types in a certain period in the study area. The calculation formula is as follows:

$$LC = \frac{\sum_{i=1}^n |U_{bi} - a_i|}{2 \sum_{i=1}^n U_{ai}} \times \frac{1}{T} \times 100\% \quad (2)$$

where  $U_{ai}$  and  $U_{bi}$  represent the areas of the specific LULC type at the start date and end date, respectively;  $T$  is the study period; and  $n$  is the number of the land use type.

### 2.2.2. Construction of Ecosystem Service Value Evaluation Model

Costanza (1997) [6] used the utility and equilibrium value theories to evaluate the global ESV for the first time. Xie (2008) [11] established the ESV equivalent per unit area of the ecosystem in China by combining the structural characteristics of China's ecosystem with the global ESV evaluated by Costanza (1997) [6]. The ESV of cities at the prefecture level and above in China was measured by Xie's (2008) [11] "Equivalent scale of ESV per unit area of terrestrial ecosystem in China". The economic value of the ESV equivalent was about 1/7 of the national average grain yield value. According to previous studies [29], when evaluating the ESV of construction land, various factors must be considered, and the calculation may be difficult, so this study would not estimate it. While estimating the ESV of unused land, the equivalent factor parameters were estimated based on the average of grassland and desert equivalent factors [30].

The economic value of grain output per unit area was calculated by actual grain yields per unit area in China's provinces, autonomous regions, and municipalities directly under the central government. The calculation formula is as follows:

$$E_a = \frac{1}{7}PQ \quad (3)$$

where  $E_a$  represents the economic value of grain yield per unit area in the study area ( $\text{yuan}/\text{hm}^2$ ), and  $P$  refers to the average value of national grain in 2018 ( $\text{yuan}/\text{kg}$ ). The average price of grain in 2018 was 2.403  $\text{yuan}/\text{kg}$ . This price was based on the average value of the national minimum purchase price of early, middle, late indica rice and the national minimum purchase price of wheat from the national development and reform commission's price monitoring center in 2018.  $Q$  is the average grain yield per unit area of each study area from 1990 to 2018 ( $\text{kg}/\text{hm}^2$ ), estimated according to the grain yield data from 31 provinces, autonomous regions, and municipalities directly under the central government in China's statistical yearbooks in 1990, 2000, 2010, and 2018 (Table 1).

However, as society develops, the degree of social development in the study area changes with time, and then ESV will also change. This study used 2018 as the base year, and it introduced the revised willingness to pay the coefficient related to social development ( $D_t$ ) to improve the accuracy of the ESV assessment model [31].  $D_t$  is calculated as follows:

$$l = \frac{2}{1 + e^{-\left(\frac{1}{E_{nt}} - 2.5\right)}} \quad (4)$$

$$E_{nt} = E_{tc} \times P_{tc} + E_{tr} \times P_{tr} \quad (5)$$

$$k = \frac{l_m}{l_n} \tag{6}$$

$$D_t = \frac{k_t}{k_{2018}} \tag{7}$$

where  $l$  is the social development stage coefficient in relation to actual willingness to pay;  $E_{nt}$  refers to the Engel coefficient of each region at year  $t$ ;  $E_{tc}$  and  $E_{tr}$  refer to the Engel coefficient of urban and rural regions at year  $t$ , respectively;  $P_{tc}$  and  $P_{tr}$  refer to the proportion of urban and rural population at year  $t$ , respectively;  $k$  is the stage coefficient of social development;  $l_m$  refers to the stage coefficient of social development of different cities, and  $l_n$  refers to the stage coefficient of the social development of China.

**Table 1.** Average grain yield per unit area by region from 1990 to 2018 (kg/hm<sup>2</sup>).

Area	1990–2018 Average Annual Grain Yield per Unit Area	Area	1990–2018 Average Annual Grain Yield per Unit Area	Area	1990–2018 Average Annual Grain Yield per Unit Area	Area	1990–2018 Average Annual Grain Yield per Unit Area
Beijing	5497.64	Shanghai	6491.62	Hubei	5655.65	Yunnan	3953.27
Tianjing	4867.92	Jiangsu	6116.74	Hunan	6003.43	Xizang	4668.72
Hebei	4788.63	Zhejiang	6077.69	Guangdong	5437.98	Shaanxi	3449.46
Shanxi	3419.26	Anhui	5035.62	Guangxi	4708.75	Gansu	3352.8
Neimenggu	3948.88	Fujian	5332.2	Hainan	4155.37	Qinghai	3288.11
Liaoning	5272.28	Jiangxi	5310.57	Chongqing	5386.97	Ningxia	4404.3
Jilin	6290.21	Shandong	5447.66	Sichuan	5520.88	Xinjiang	5699.57
Heilongjiang	4685.64	Henan	5303.36	Guizhou	3948.57		

Combined with the revised willingness to pay the coefficient related to social development ( $D_t$ ), we constructed an ESV evaluation model suitable for cities at the prefecture level and above in China [31]. The calculation formula is as follows:

$$ESV = \sum_{i=1}^m \sum_{j=1}^n A_i \times M_{ij} \times E_a \times D_t \tag{8}$$

where ESV is the total value of ecosystem services in the study area (10<sup>10</sup> yuan);  $A_i$  is the area of class  $i$  land use type (km<sup>2</sup>);  $M_{ij}$  is the table value of the equivalent factor corresponding to  $j$  ecosystem service function of class  $i$  land use type (Table 2);  $m$  is the number of ecosystem types, and  $n$  is the number of ecosystem service function items;  $E_a$  is the economic value of grain output per unit area (yuan/hm<sup>2</sup>);  $D_t$  is the coefficient of the social development stage after the introduction of the Engel coefficient and modification by the logistic regression model.

**Table 2.** Equivalent value per unit area of ecosystem services in China (yuan/hm<sup>2</sup>.a).

Type	Sub-Type	Farmland	Woodland	Grassland	Water Body	Unused Land	Construction Land
Provisioning services	Food production	1.00	0.33	0.43	0.53	0.23	0.00
	Raw material	0.39	2.98	0.36	0.35	0.20	0.00
	Gas regulation	0.72	4.32	1.50	0.51	0.78	0.00
Regulating services	Climate regulation	0.97	4.07	1.56	2.06	0.85	0.00
	Hydrology regulation	0.77	4.09	1.52	18.77	0.80	0.00
	Waste treatment	1.39	1.72	1.32	14.85	0.79	0.00
Supporting services	Soil conservation	1.47	4.02	2.24	0.41	1.21	0.00
	Biodiversity maintenance	1.02	4.51	1.87	3.43	1.14	0.00
Cluture service	Esthetic landscape provision	0.17	2.08	0.87	4.44	0.56	0.00
	Total	7.90	28.12	11.67	45.35	6.53	0.00

### 2.2.3. Hot-Spot Analysis

The Getis–Ord  $G_i^*$  can be used to describe the spatial agglomeration degree of ESV. The hot and cold spots represent statistically significant high-value and low-value spatial agglomeration of ESV and its changes [32]. The Getis–Ord  $G_i^*$  index is calculated as [33].

$$G_i^*(d) = \frac{\sum_{j=1}^n w_{ij}x_j - \bar{X} \sum_{j=1}^n w_{ij}}{S \sqrt{[n \sum_{j=1}^n w_{ij}^2 - (\sum_{j=1}^n w_{ij})^2]/(n-1)}} \tag{9}$$

$$S = \sqrt{\frac{\sum_{j=1}^n x_j^2}{n} - (\bar{X})^2} \tag{10}$$

where  $x_j$  is the ESV of unit  $j$ ,  $\bar{X}$  is the average value of ESV,  $W_{ij}$  refers to the spatial weight coefficient between geospatial units, and  $n$  is the total number of units.  $G_i^*$  is represented by the Z-value. For positive z-scores, with statistically significant positive values, the higher the Z-score is, the more intense the clustering of high-values (hot spots) will be. Similarly, for statistically significant negative z-scores, the lower the z-score is, the more intense is the cluster of low-values (cold spots) will be.

### 2.2.4. Barycenter Model

The barycenter model is an effective tool for analyzing how spatial variables change over time [34]. We introduced the model to reveal the spatial evolution characteristics of ESV. The center of gravity of ESV in China has changed over the study period, and its movement represents the spatial trajectory of ESV change in China. The calculation formula is as follows:

$$\bar{X} = \frac{\sum_{i=1}^n x_i w_{it}}{\sum_{i=1}^n w_{it}}, \bar{Y} = \frac{\sum_{i=1}^n y_i w_{it}}{\sum_{i=1}^n w_{it}} \tag{11}$$

$$D = \sqrt{(\bar{x}_{t2} - \bar{x}_{t1})^2 + (\bar{y}_{t2} - \bar{y}_{t1})^2} \tag{12}$$

where  $\bar{X}$  and  $\bar{Y}$  are the longitude and latitude of the barycenter, respectively;  $x_i$  and  $y_i$  are the longitude and latitude of unit  $i$ , respectively;  $w_{it}$  is the ESV of unit  $i$  at year  $t$ ; and  $D$  is the moving distance of the center of gravity.

### 2.2.5. Geographical Detector Model

Wang (2016) [35] proposed the Geographical detector model, a statistical tool for detecting spatial differentiation caused by geographical elements and revealing the driving force behind it. Without excessive assumptions, this method can overcome the limitations of traditional statistical analysis methods. This method, which has been widely used in the fields of social economy and environment, can not only detect the spatial differentiation of a single factor but can also assess the interaction of multiple factors [18,36,37]. To detect the driving factors influencing the spatial difference of ESV in the study area, this study primarily used the two modules of factor and interaction detection in the geographic detector model. The calculation formula is as follows:

$$q = 1 - \frac{\sum_{h=1}^L N_h \sigma_h^2}{N \sigma^2} \tag{13}$$

where  $q$  is the detection index of the influencing factors of the spatial differentiation of ESV in China, and the interval is [0, 1]. The greater the value of  $q$  is, the stronger the

heterogeneity of the spatial stratification will be. Conversely, the lesser the value of  $q$  is, the randomness of the spatial distribution will be stronger. The value of  $q$  is 0, indicating that the factor has no influence on ESV;  $N$  and  $\sigma^2$  are the sample size and variance, respectively;  $N_h$  and  $\sigma_h^2$  are the secondary sample size and variance, respectively; and  $h = 1, 2, \dots, L$ , which is the stratification of variable  $Y$  or factor  $X$ .

### 3. Results

#### 3.1. Change in Land Use from 1990 to 2018

On the basis of the land use data of four periods in 1990, 2000, 2010, and 2018, the land use transfer matrix in China was calculated, and the transfer chord diagram between different land use types was created (Figure 2). During the study periods of 1990–2000, 2000–2010, 2010–2018, and 1990–2018, the evolution characteristics of various land use types in the study area were analyzed. The results showed that throughout each time, the area of each land type in the study area changed to varying degrees. Woodland and grassland were always the two primary land types. Specifically, the change in grassland net area always showed a decreasing trend. The net area declined by 12.71% across the study period. Especially from 2010 to 2018, the net area of grassland dropped by 11.4% and mostly shifted to farmland, woodland, and unused land; Over the study period, the change in woodland was relatively moderate, with a steady decreasing trend from 1990 to 2000, followed by a slowly increasing trend from 2000 to 2018; From 1990 to 2000, the net area of farmland increased by 1.61%, whereas from 2000 to 2018, it began to slowly decrease, with most of the land being moved to woodland, grassland, and construction land; From 1990 to 2010, the unused land and water body changed steadily, whereas the increase from 2010 to 2018 showed an increasing trend, with increases of 11.39% and 6.07%, respectively; The change in construction land was the most significant, and the change rate continued to increase throughout the three study periods. The change rate of construction land reached 34.95%, particularly from 2010 to 2018.

According to the land use data of each year, Formulas (1) and (2) were used to calculate the single and comprehensive dynamic degrees in 1990–2000, 2000–2010, 2010–2018, and 1990–2018, respectively. The area of each land type in the study area changed to varying degrees in each period, as shown in Tables 3 and 4. From the perspective of single dynamic degree, the land use dynamic degree of grassland was always negative, with the greatest decline range (1.17%) between 2010 and 2018. Farmland and woodland change rates were relatively slow, but overall showed an increasing trend, with increases of  $1.50 \times 10^4 \text{ km}^2$  and  $2.33 \times 10^4 \text{ km}^2$ , respectively. The land use dynamic degree of farmland showed an increasing trend from 1990 to 2000, and then decreased by a tiny margin in 2000–2010 and 2010–2018, and the decreasing range continued to increase. The land use dynamic degree of woodland was always less than 0.1% in each period, and the change range was not obvious; The water body kept increasing throughout the study period. Especially from 2000 to 2010, The land use dynamic degree of water body reached 0.53%; The unused land changed in a slowly decreasing trend from 1990 to 2010, and then it increased slightly from 2010 to 2018; During the study period, the area of construction land continued to grow rapidly. From 1990 to 2018, the dynamic degree of land use in the whole study period from 1990 to 2018 increased by 2.50%, with a total increase of  $10.72 \times 10^4 \text{ km}^2$ . This discovery was mostly due to population growth, urban development, and other factors, which resulted in a progressive rise in the amount of construction land. The comprehensive land use dynamics were always less than 0.05% from 1990 to 2010, but this changed greatly from 2010 to 2018, reaching 0.36%.

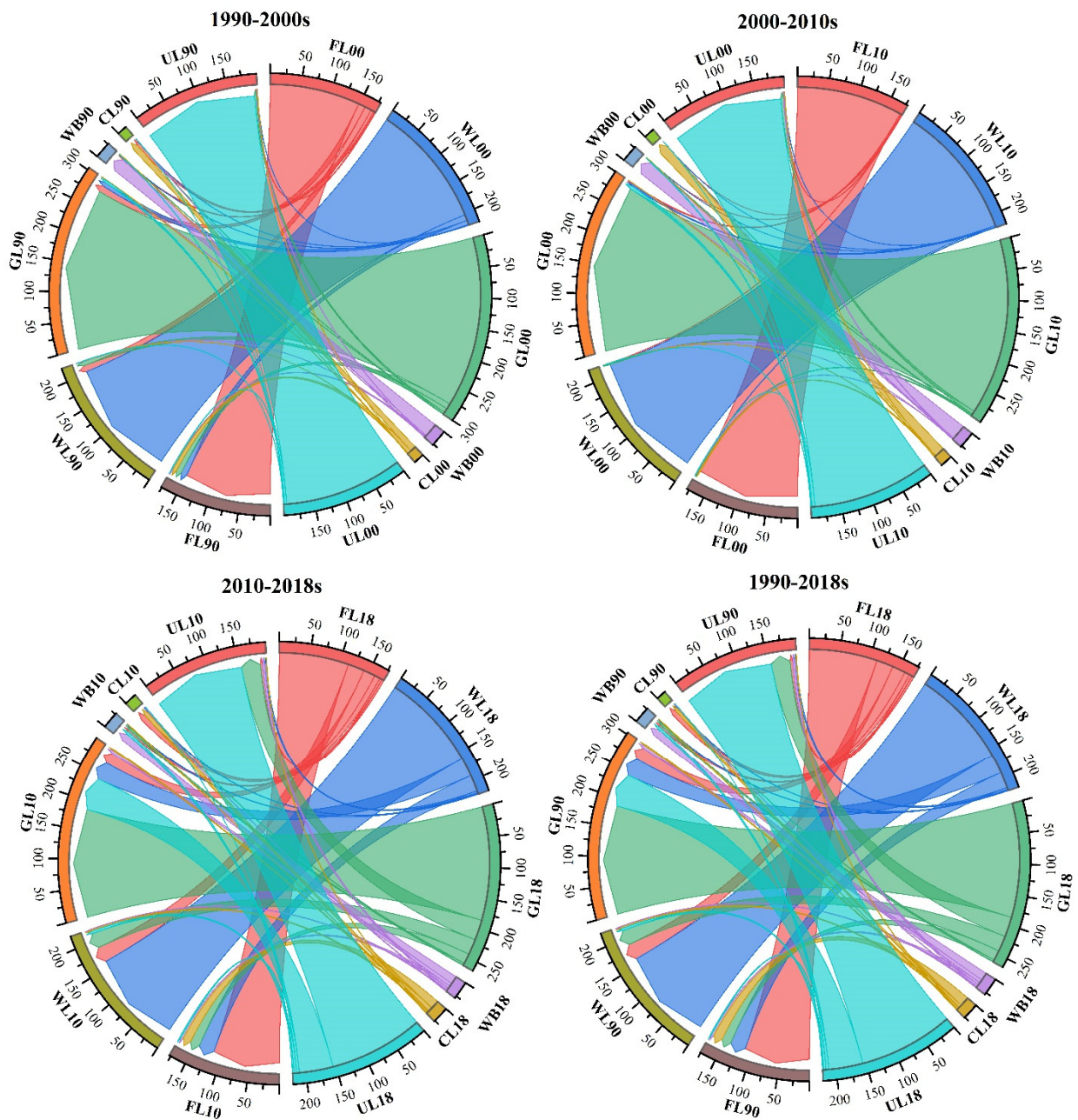


**Figure 2.** Chord diagram of land use type transfer in China from 1990 to 2018 (Note: FL: Farmland, WL: Woodland; GL: Grassland; WB: Water body; CL: Construction land; UL: Unused land).

**Table 3.** Area change of different land use types in China from 1990 to 2018 ( $10^4 \text{ km}^2$ ).

	Farmland	Woodland	Grassland	Water Body	Construction Land	Unused Land
1990–2000	2.89	−1.18	−3.34	0.27	1.38	−0.04
2000–2010	−0.50	1.30	−0.42	1.37	2.83	−0.07
2010–2018	−0.90	2.21	−34.97	0.43	6.51	22.20
Net change in 1990–2018	1.50	2.33	−38.74	2.06	10.72	22.10

**Table 4.** Dynamic changes of land use in China from 1990 to 2018 (%).

	Single Land Use Change/%						Comprehensive Land Use Change
	Farmland	Woodland	Grassland	Water Body	Construction Land	Unused Land	
1990–2000	0.16	−0.05	−0.11	0.11	0.90	−0.002	0.05
2000–2010	−0.03	0.06	−0.01	0.53	1.69	−0.003	0.03
2010–2018	−0.05	0.10	−1.17	0.16	3.33	1.11	0.36
1990–2018	0.03	0.04	−0.46	0.29	2.50	0.40	0.41

### 3.2. Spatiotemporal Variation of ESV

#### 3.2.1. Spatiotemporal Variation of ESV from 1990 to 2018

According to the results of the ESV evaluation model, the total ESV in the study area in 1990, 2000, 2010, and 2018 was 23.54, 22.53, 22.64, and 21.97 trillion yuan, respectively. During the study period, the total amount of ESV decreased by 6.67%, with an average yearly decline rate of 0.24%. Figure 3 shows how the ESV produced by various land use types and ecosystem subservice structure alterations varied. From the perspective of various land use types, the ESV produced by woodland was the largest, followed by grassland, farmland, unused land, and water body. The ESV generated by farmland and unused land increased by 3.50% and 7.41%, respectively, whereas the ESV of other land types decreased, especially grassland, which decreased by a total of 23.80%. From the perspective of various ecosystem subservice structures, the ESV generated by the four ecosystem service structures was in the following order: regulating services > supporting services > provisioning services > cultural services. The change trend was consistent across the three research periods, showing a trend of initially decreasing, then increasing, and finally decreasing. During the whole study period, supporting services saw the greatest decrease in ESV, with a total decrease of 7.35%, whereas provisioning services experienced the least decrease, with a total decrease of 4.79%.

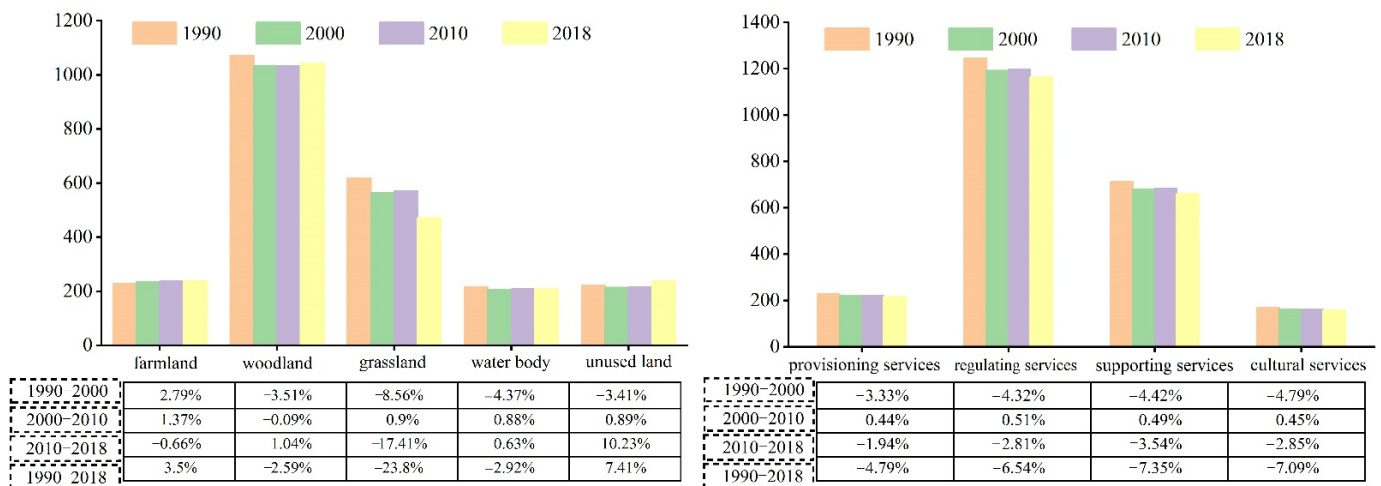


**Figure 3.** ESV and its change rate of different land use types in China from 1990 to 2018.

ESV was divided into five levels (Figure 4) using the natural breakpoint method in ArcGIS 10.2: extremely low ESV ( $<3.48 \times 10^{10}$  yuan), low ESV ( $3.48 \times 10^{10}$ – $8.27 \times 10^{10}$  yuan), medium ESV ( $8.47 \times 10^{10}$ – $16.68 \times 10^{10}$  yuan), high ESV ( $16.68 \times 10^{10}$ – $45.77 \times 10^{10}$  yuan), and extremely high ESV ( $>45.77 \times 10^{10}$  yuan). In the four periods, the spatial distribution of ESV was largely similar. The high and extremely high ESV were primarily distributed in Tibet, Xinjiang, and Neimenggu, due to the huge distribution of grassland in the western region and the large ESV produced by grassland. The medium, low, and extremely low ESV were primarily distributed in the central, southern, and eastern coastal regions due

to the large amount of farmland in these areas which generated less ESV than woodland and grassland.

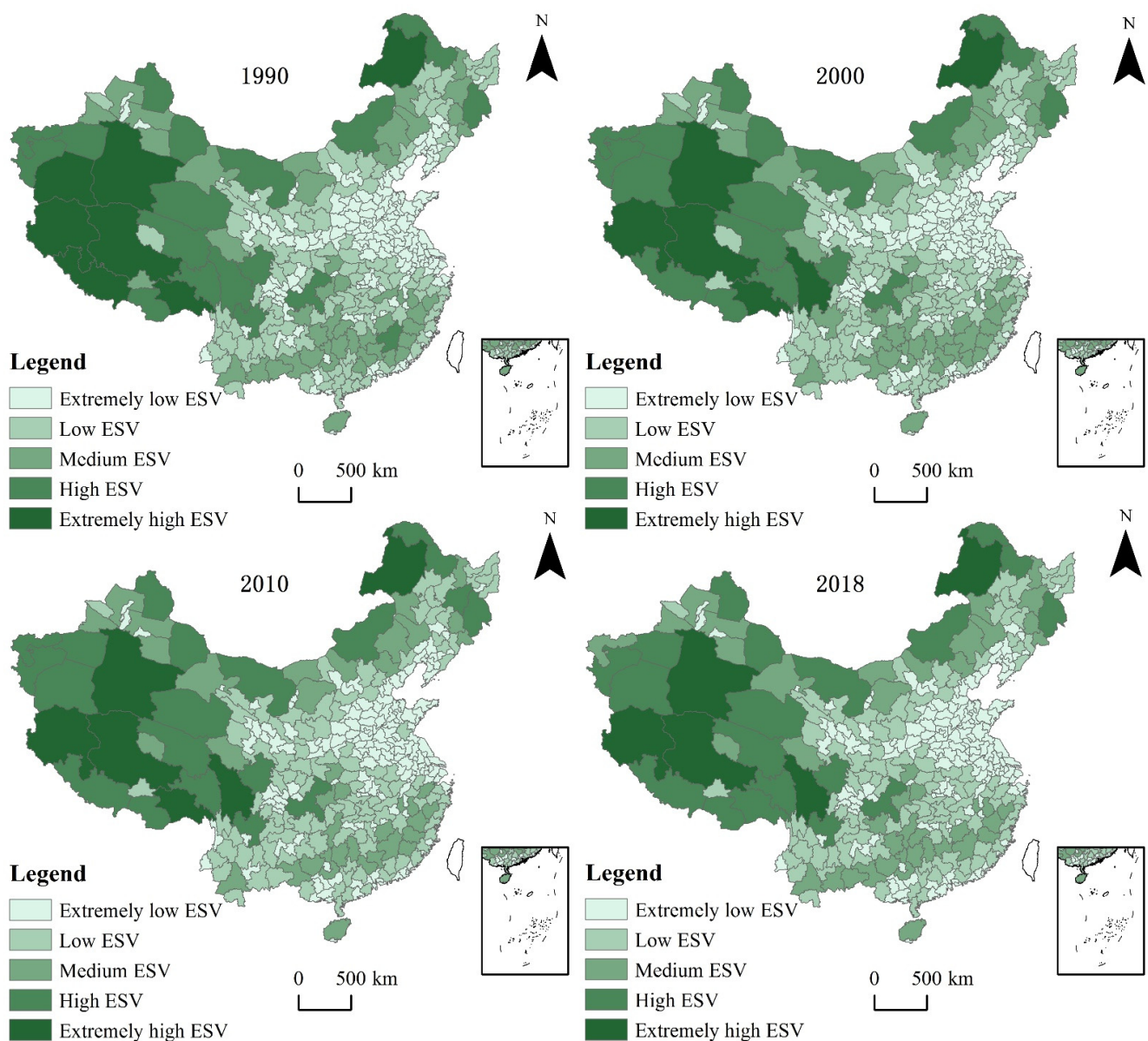


**Figure 4.** Spatial distribution characteristics of ESV in the study area.

### 3.2.2. Evolution Characteristics of Cold and Hot Spots of Ecosystem Service Value

With the help of the hot spot analysis tool in ArcGIS 10.2, this study conducted a hot spot analysis on the ESV in 1990, 2000, 2010, and 2018 (Figure 5). In the four periods, the distribution of cold spots and hot spots in the study area was relatively consistent, and both were relatively concentrated. The hot spots were primarily distributed in the whole region of Tibet, parts of Xinjiang, Heihe City and Tahe County in northeast Heilongjiang Province, and Hailar City in Neimenggu. The cold spots were primarily distributed in the eastern region. The sub-hot and sub-cold spots were sporadically scattered. The variations in cold and hot spots were less noticeable with time. The number of sub-cold spots has increased over time, but they were still mostly distributed around the cold spots. The distribution of sub-hot spots varied with time, and the distribution areas were different.

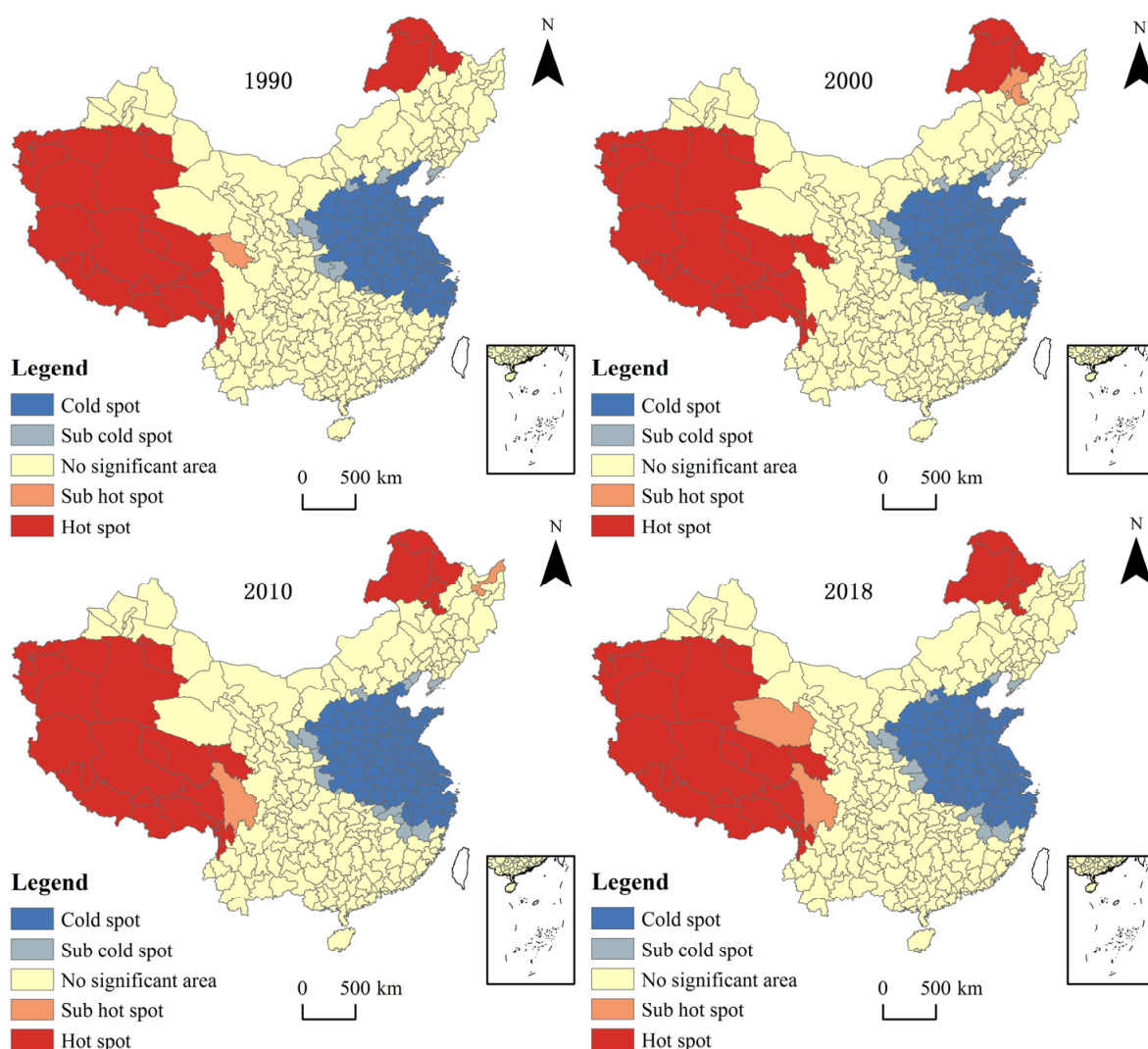


**Figure 5.** Spatial distribution of cold and hot spots of ESV in China from 1990 to 2018.

To further explore the temporal and spatial distribution characteristics of ESV changes in China from 1990 to 2018, the cold and hot spot map in the change of ESV in the study area was described again with the use of a hot spot analysis tool (Figure 6). From 1990 to 2000, the cold spots were primarily distributed in Tibet, the sub-cold spots were distributed in Yuxi City, the hot spots were primarily distributed in north China, and the sub-hot spots were widely distributed in north China, the eastern coast, and the southwest; From 2000 to 2010, the cold spots were primarily distributed in the south, whereas the sub-cold spots increased slightly, primarily distributed around the cold spot area. In comparison with the stage from 1990 to 2000, the number of hot spots increased significantly, and the degree of aggregation also increased, mostly distributed in Qinghai, Sichuan, and Heilongjiang Province. The number of sub-hot spots decreased significantly and scattered around the hot spots; From 2010 to 2018, the regional distribution of cold and hot spots changed significantly. Cold spots were mainly distributed in Tibet and some areas of Heilongjiang and Inner Mongolia in the northeast. The number of sub cold spots decreased, with the majority of them concentrated in Mudanjiang City. The spatial distribution of hot spots was concentrated mostly in the central and southwest areas. The number of sub hot spots slightly increased compared with the previous stage, and was primarily distributed in the central area.

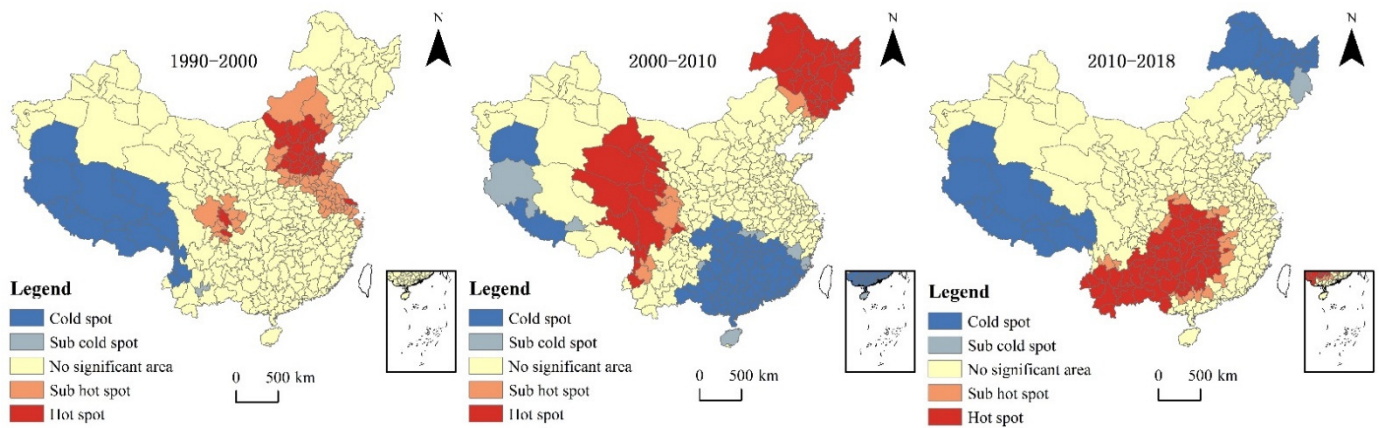


**Figure 6.** Spatial distribution of cold and hot spots of ESV changes in China from 1990 to 2018.

### 3.2.3. Barycenter Evolution of Ecosystem Service Value

According to the barycenter model in Formulas (6) and (7), the change in China’s ESV center of gravity trajectory was calculated. As shown in Figure 7, the center of gravity of ESV was primarily distributed in Pingliang City and Dingxi County of Shaanxi Province from 1990 to 2018, and the overall change difference was obvious, with an “S”-shaped trend. From 1990 to 2000, the center of gravity of ESV in the study area migrated by 64.38 km in the direction of 28° north by east. During this period, ESV changed significantly and showed a decreasing trend, with a total decrease of 1.01 trillion yuan; From 2000 to 2010, it continued to migrate by 47.26 km in the direction of 67° northeast. During this period, ESV changed slowly, mostly increasing, with a total increase of 0.11 trillion yuan; From 2010 to 2018, it migrated by 36.24 km in the direction of 34° southeast. During this period, ESV showed a decreasing trend, with a total decrease of 0.67 trillion yuan.

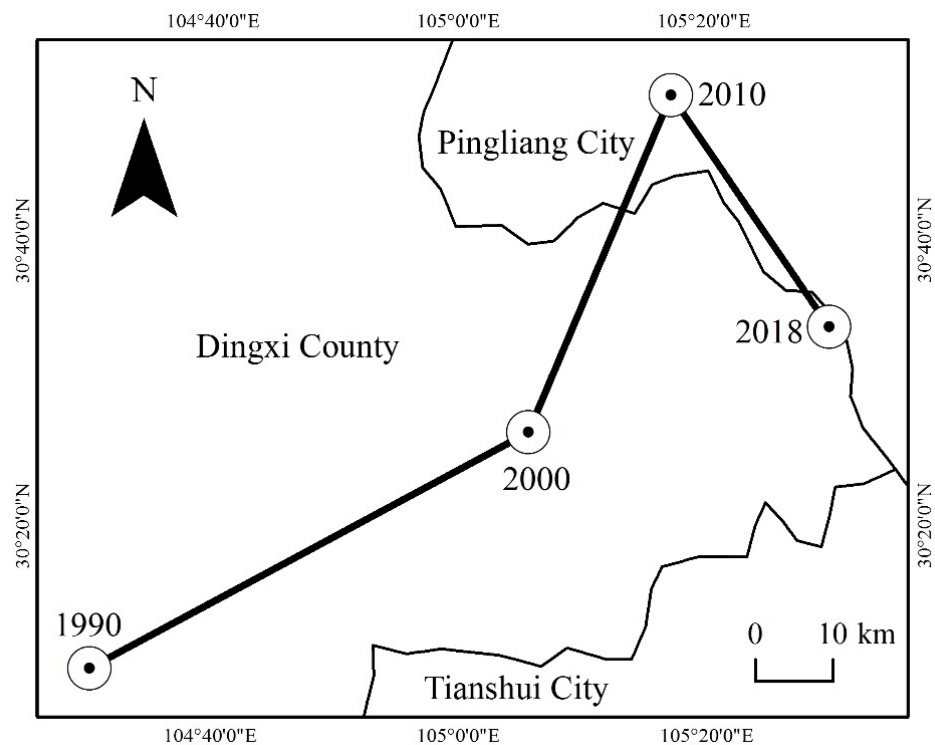


**Figure 7.** Barycenter evolution trajectory of ESV.

### 3.3. Driving Factors of Regional Differences in Ecosystem Service Value

Taking 2000 and 2018 as examples, a total of nine driving factors were selected from the two aspects of physical geography and social economy. The ESV was used as the dependent variable of the geographical detector. The independent variables were the slope (X1), elevation (X2), average annual temperature (X3), annual precipitation (X4), NDVI (X5), population density (X6), GDP (X7), construction land intensity (X8), and distance from road (X9). The influence degree of each driving factor on the spatial differentiation characteristics of ESV in the study area, as well as the interaction characteristics between the driving factors, were described using the geographical detector's factor detection and interactive detection functions. China spanned a huge area from east to west and north to south, and different natural and socioeconomic factors influenced different regions in various ways. This paper divided the study area into six regions (i.e., northeastern region, north China, east China, south central region, northwest region, and southwest region) for further analysis to better detect the effects of various driving factors on the temporal and spatial differentiation of ESV in the study area. As shown in Table 5, the influence of each driving factor on the spatial differentiation characteristics of ESV in the study area was mostly explained using the Q statistic. From a national scale, the  $p$  value of all the driving factors, which were all significant characteristics, was less than 0.01 during the study period. The main natural factors that influenced the spatial differentiation of ESV were elevation (X2) and average annual temperature (X3). The main social factors that influenced the spatial differentiation of ESV were always population density (X6) and distance from road (X9). Simultaneously, the influence of construction land intensity (X8) on the spatial differentiation of ESV changed significantly from 0.19 to 0.33 between 2000 and 2018. The effects of other driving factors on the spatial differentiation of ESV did not change significantly over time. This result was mostly due to the wide latitude and longitude spans of the various regions in China, as well as the fast social and economic growth with the passage of time. Moreover, construction land encroached on other ecological lands, making construction land intensity (X8) one of the main driving factors of ESV spatial differentiation. From the regional scale, the main driving factors influencing the spatial differentiation characteristics of ESV were different. The most important socioeconomic factors for the spatial differentiation of ESV in the northeast region and north China were population density (X6), construction land intensity (X8), and distance from road (X9). The annual average temperature (X3) had a significant influence on the spatial differentiation of ESV in the northeast region in 2000, but not in 2018. The Q statistic of the annual average temperature (X3) on ESV in north China between 2000 and 2018 was 0.74, indicating significant characteristics; In east China and the south central region, slope (X1), population density (X6), and construction land intensity (X8) had the strongest explanations. The influence of NDVI (X5) increased over time, whereas that of distance from road (X9) on the spatial differentiation of ESV in the two regions was insignificant; In the northwest region, the main driving factors were NDVI (X5) and distance from road (X9), with the annual precipitation (X4) and construction land intensity (X8) gradually increasing their explanatory strength for ESV over time; Natural factors such as elevation (X2), average yearly temperature (X3), and NDVI (X5) exhibited significant influence on the ESV of the southwest region, in addition to distance from road (X9), which explained the largest degree of spatial differentiation of ESV.

The interactive detection results showed that bi-enhanced or nonlinear enhanced effects were primarily interaction types between natural and socioeconomic factors. This finding indicates that the spatial differentiation of ESV in the study area was caused by the interaction of multiple driving factors, rather than being purely influenced by one factor. From a national scale (Figure 8), the interaction degree between slope (X1) and distance from road (X9) was the largest, with an interaction intensity of 0.74. The influence of the interaction between distance from road (X9) and other factors on the spatial differentiation of ESV was greater than 0.60, and the interaction between distance from road (X9) and natural factors was significantly greater than the interaction between distance from road

(X9) and socioeconomic factors. From the regional scale, we listed the top three dominant interactions of influence of different driving factors on the spatial differentiation of ESV in each region (Table 6). Overall, construction land intensity (X8) and distance from road (X9) had the most significant interactions with other factors, especially with natural factors. Thus, the interactive effect between natural and socioeconomic factors further enhanced the effect on the spatial differentiation of ESV. Specifically, in the northeast, northwest, and southwest regions, the main interactions came from the interaction between natural factors and distance from road (X9) in 2000 and 2018. The interaction between elevation (X2) and distance from road (X9) in the northeast region was always the largest; The interaction between distance from road (X9) and altitude (X2) and the interaction between distance from road (X9) and annual average temperature (X3) in Northwest China always ranked in the top two. In the southwest region, the interactions between distance from road (X9) and natural factors were above 0.90, and the interaction intensity was relatively large. The primary interactions in north China, east China, and the south central region were produced by the interaction of natural factors and the intensity of development land (X8). During the research period, the top three interactions in north China were primarily the interaction intensity among construction land intensity (X8), with elevation (X2), annual average temperature (X3), and NDVI (X5), all of which had interaction strengths over 0.92; In east China and the south central region, the interaction between slope (X1) and construction land intensity (X8) was the strongest, and the interaction between them kept growing as the years passed.

**Table 5.** Q statistic of the driving factors of ESV in different regions in 2000 and 2018.

		X1	X2	X3	X4	X5	X6	X7	X8	X9
Nation	2000	0.10 **	0.28 **	0.29 **	0.08 **	0.23 **	0.31 **	0.05 **	0.19 **	0.58 **
	2018	0.11 **	0.28 **	0.32 **	0.16 **	0.25 **	0.35 **	0.06 **	0.33 **	0.58 **
Northeastern region	2000	0.16	0.35	0.48 *	0.01	0.22 *	0.33 *	0.01	0.43 **	0.41 *
	2018	0.18	0.38	0.34	0.01	0.12	0.36 **	0.05	0.46 *	0.38 *
North China	2000	0.07	0.11	0.74 **	0.04	0.12	0.4 *	0.08	0.44 **	0.73 **
	2018	0.07	0.11	0.74 **	0.1	0.13	0.45 **	0.13	0.79 **	0.73 **
East China	2000	0.46 **	0.26 *	0.04	0.44 **	0.15 **	0.48 **	0.04	0.48 **	0.02
	2018	0.44 **	0.22	0.03	0.39 **	0.4 **	0.44 **	0.09	0.61 **	0.02
South central region	2000	0.43 **	0.41 **	0.07	0.18 **	0.2 **	0.55 **	0.02	0.57 **	0.04
	2018	0.43 **	0.44 **	0.02	0.22 **	0.49 **	0.51 **	0.08	0.62 **	0.05
Northwest region	2000	0.18	0.06	0.08	0.13 *	0.26 *	0.21 **	0.07	0.16 *	0.57 **
	2018	0.19	0.07	0.13	0.24 **	0.36 **	0.23 **	0.09	0.26 **	0.61 **
Southwestern region	2000	0.1	0.58 **	0.65 **	0.52 *	0.76 **	0.39 **	0.19	0.03	0.87 **
	2018	0.11	0.57 **	0.65 **	0.51 *	0.67 **	0.42 **	0.51 **	0.16 *	0.81 **

Note: \*:  $p < 0.05$ ; \*\*:  $p < 0.01$ .



**Figure 8.** Result of driving factor interaction detection in a national scale in 2000 and 2018.

**Table 6.** Dominant interactions between two variables in different regions.

		Dominant Interaction 1	Dominant Interaction 2	Dominant Interaction 3
Northeastern region	2000	X2 ∩ X9 (0.855)	X7 ∩ X9 (0.825)	X8 ∩ X9 (0.786)
	2018	X2 ∩ X9 (0.858)	X7 ∩ X9 (0.849)	X2 ∩ X7 (0.746)
North China	2000	X5 ∩ X8 (0.954)	X5 ∩ X9 (0.935)	X3 ∩ X9 (0.927)
	2018	X3 ∩ X8 (0.989)	X5 ∩ X8 (0.984)	X2 ∩ X8 (0.983)
East China	2000	X1 ∩ X8 (0.667)	X4 ∩ X6 (0.665)	X1 ∩ X4 (0.660)
	2018	X7 ∩ X8 (0.732)	X1 ∩ X8 (0.690)	X4 ∩ X8 (0.661)
South central region	2000	X1 ∩ X8 (0.694)	X2 ∩ X8 (0.684)	X1 ∩ X5 (0.679)
	2018	X7 ∩ X8 (0.751)	X1 ∩ X8 (0.750)	X3 ∩ X8 (0.736)
Northwest region	2000	X2 ∩ X9 (0.865)	X3 ∩ X9 (0.865)	X4 ∩ X9 (0.849)
	2018	X3 ∩ X9 (0.867)	X2 ∩ X9 (0.865)	X5 ∩ X9 (0.858)
Southwestern region	2000	X4 ∩ X9 (0.957)	X1 ∩ X9 (0.954)	X5 ∩ X9 (0.925)
	2018	X5 ∩ X9 (0.928)	X1 ∩ X9 (0.924)	X4 ∩ X9 (0.908)

#### 4. Discussion

##### 4.1. ESV Dynamic Change in Response to LUCC in China

The ESV of each Chinese region was calculated using Xie's (2008) [11] ESV equivalent per unit area of the ecosystem. Simultaneously, the sensitivity index was used to reflect the change of ESV caused by the change in ESV coefficient by 1% (See References [38,39] for details). The results showed that the ESV has decreased by 1.57 trillion yuan, with an average annual decline rate of 0.24%. During the study period, the sensitivity indexes of different land use types have been in a stable state and were less than 1 (Figure 9), indicating that the ESV coefficient was reasonable in the study area. In addition, the sensitivity index of different land use types in the study area was in the following order from high to low: woodland > grassland > farmland > unused land > water body. Woodland and grassland contributed the most ESV, whereas unused land and water body contributed the least. Therefore, to ensure the stability and coordination of ESV, we should improve the protection of woodland and grassland. From the perspective of the spatial distribution of ESV, we found an obvious phenomenon of high and low value aggregation of ESV. The high and extremely high ESV was mainly distributed in the northwest region with more grassland. The low ESV was mainly distributed in the central region and the eastern coastal region; this part of the region had rapid economic development and serious occupation of ecological resources. The center of gravity of ESV in the study area was always distributed in Shaanxi Province, and continued to move north by east with the passage of time, generally in an "S"-shaped trend. The ESV was affected by changes in land use. To maintain the security and stability of ecosystem service capacity, relevant departments should properly adjust the land use structure and strengthen the ecological land occupation and compensation mechanism in each region.

##### 4.2. Impact Factors on ESV Distribution

The spatial differentiation of ESV was affected to some extent by the interaction between human activities and the ecological environment [40]. Exploring the impact mechanism of the spatial differentiation of ESV, which was of great significance to China's ecosystem management and ecological pattern optimization, could help in further explaining the generating mechanism of ecological problems.

This study quantitatively analyzed the relative importance of the driving factors to the ESV and the degree of interaction among driving factors in the national and regional scales. The results showed that the primary driving factors affecting the spatial differentiation of ESV were different in the whole nation and different regions. From a national scale, elevation (X2), average annual temperature (X3), population density (X6), and distance from road (X9), were the primary driving factors affecting the spatial differentiation of ESV, especially distance from road (X9). From the different regional scales, the driving factors affecting the spatial differentiation of ESV in the northeast, north, east, and south

central regions were mainly socioeconomic factors, such as population density (X6) and distance from road (X9). In northwest and southwest regions, the primary driving factor was not only the distance from road (X9), but also the annual average temperature (X3), NDVI (X5), and other natural factors. At the same time, the influence of construction land intensity (X8) on the spatial differentiation of ESV also increased over the years, and it has recently become one of the major driving factors affecting the spatial differentiation of ESV in the nation scale and different regional scales. The interaction between driving factors had a greater influence on ESV than that of a single factor, and the interaction between socioeconomic and natural factors had a greater influence on the spatial differentiation of ESV. In particular, the interaction among construction land intensity (X8), distance from road (X9), and other natural factors was always stronger than that with socioeconomic factors. This finding was made because, as the social economy develops, the intensity of human activities has increased, the speed of urban expansion also increases, and some irrational reclamation and construction has occupied green vegetation land, such as farmland, woodland, and grassland, thereby putting great pressure on the ecosystem's stability [41]. Therefore, China should properly control the rate of urbanization and optimize the land use structure. While focusing on the coordinated development of ecological and economic construction, more ecological protection and restoration projects must be implemented to increase vegetation coverage and mitigate water and soil loss, thereby ensuring the stability of the ecosystem [42,43].

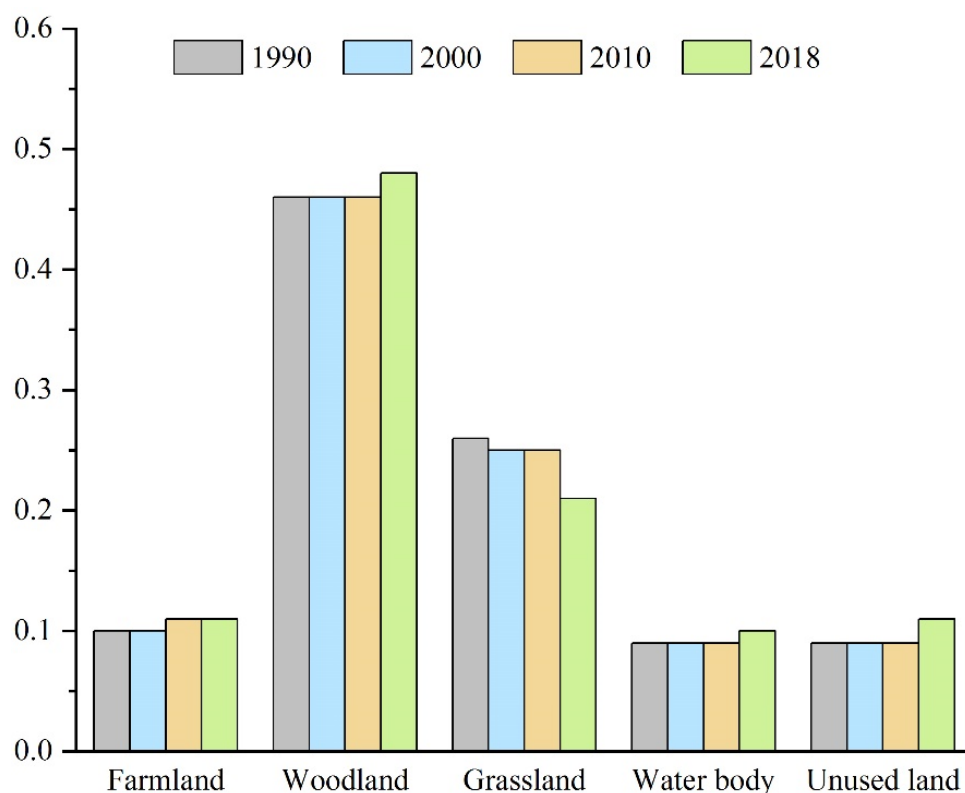


**Figure 9.** Sensitivity index of ESV.

#### 4.3. Limitations and Improvement

Xie (2008) [11] created the ESV equivalent per unit area of the ecosystem in China, which has been widely used by Chinese scholars in the assessment of ESV [44,45]. The revised willingness to pay coefficient related to social development ( $D_i$ ) was introduced in our paper based on this table to modify the evaluation model of ESV. However, due to the large span from north to south and east to west, significant differences were observed in the geographical environments of the various regions in the study area. This paper did

not formulate the ESV equivalent per unit area of terrestrial ecosystem suitable for each region according to the actual situation of each region, resulting in a certain deviation in calculation. Furthermore, while using the geographical detector model to analyze the driving mechanism of ESV spatial difference, this study did not consider the relevant policy factors. At the same time, due to the limitations of the model's own characteristics, it could not accurately describe the spatial characteristics of each driving factor's influence on ESV. In the future, we will select appropriate policy factors and use a geographically and temporally weighted regression model to advance our arguments.

## 5. Conclusions

(1) During the study period, grassland always showed a decreasing trend, with a total decline of  $38.74 \times 10^4 \text{ km}^2$ , due to the large quantity of grassland transferred to farmland, woodland, and unused land. Farmland increased from 1990 to 2000, then slightly decreased from 2000 to 2018, but it kept growing throughout the study period, with a net area increase of  $1.5 \times 10^4 \text{ km}^2$ . The change in woodland in each research stage was not obvious. The land use dynamic degree of the water body was always positive, increasing by  $2.06 \times 10^4 \text{ km}^2$  throughout the study period. From 1990 to 2010, the amount of unused land decreased, but increased from 2010 to 2018, with an overall increase. Construction land changed the most throughout the study period, and the dynamic degree of construction land was always positive, with an increase of  $10.72 \times 10^4 \text{ km}^2$ , and farmland was the largest source of growth of construction land. The comprehensive dynamic degree of land use has also increased over time, especially from 2010 to 2018.

(2) From 1990 to 2018, the high ESV was mostly in the western region. The total amount of ESV decreased by 6.67% over the last three decades, with an average yearly decline rate of 0.24%. From the perspective of different land use types, the ESV generated by woodland and grassland was the main part of the total ESV. During the study period, farmland and unused land showed an increasing trend, whereas other land use showed a decreasing trend, especially grassland. From the perspective of different ecosystem subservice structures, regulating services produced the most ESV, whereas cultural services produced the least. Supporting services decreased the most during the study period, with a total decrease of 7.35%. The distribution of ESV cold and hot spots in the study area was relatively consistent in 1990, 2000, 2010, and 2018. The hot spots were mostly concentrated in the northeast and northwest regions, whereas the cold spots were mostly concentrated in east China. During the study period, the numbers of both remained relatively consistent. The number of sub-cold spots increased with time, mainly in the vicinity of cold spots. The distribution of sub-hot spots changed with time. The center of gravity model showed that ESV's center of gravity was always distributed in Shaanxi Province, and it continues to migrate northeast of China in an "S"-shaped trend.

(3) The results of the Geographical detector model revealed that the spatial difference of ESV in China was driven by a combination of natural and socioeconomic factors, and that the influence of different driving factors on ESV in the study area was significantly different. From a national scale, the ESV is mostly affected by the distance from the road (X9). From the regional scale, the primary factors affecting the spatial differentiation of ESV were different. Socioeconomic factors dominated in the northeast area, north China, east China, and the central south region. Distance from road (X9) was the most important factor in the northwest and southwest areas (X9). In southwest China, natural factors such as annual average temperature (X3) and NDVI (X5) were also primary factors. At the same time, the spatial differentiation of ESV was the result of the interaction of multiple driving factors rather than a single factor. In particular, the interaction among construction land intensity (X8), distance from road (X9), and other driving factors was significantly enhanced.

(4) By analyzing the spatiotemporal differentiation of China's ESV and exploring the driving mechanism of ESV at national and regional scales, this paper proposed some policy implementation suggestions for environmental conservation in China. First, we should pay more attention to the areas of low ESV, especially in the central and eastern coastal

regions, where fast economic growth and high degree of urbanization have transformed a huge quantity of ecological land into construction land. For these areas, some ecological land for specific applications should be earmarked, and protective measures should be taken to avoid being occupied by construction land. Simultaneously, land consolidation for residential areas and related infrastructure in rural areas should be promoted. Second, some areas with high ESV, especially in northwest China, have more woodlands and grasslands, which produce more ESV. However, the effects of human activities on these areas continues to increase over time. Indiscriminate land reclamation and overgrazing have led to the destruction of woodland and the degradation of grasslands. For these areas, to limit unreasonable human activities, various ecological protection measures should be implemented. For example, policy subsidies should be offered to relevant employees to encourage them to return farmland to forest and grassland.

**Author Contributions:** Conceptualization, X.W. and L.Z.; Data collection, L.Z., P.C., M.X. and H.W.; Data processing, X.W., L.Z., P.C. and M.X.; writing—original draft preparation and review and editing, X.W. and L.Z. All authors have read and agreed to the published version of the manuscript.

**Funding:** This research was funded by the National Natural Science Foundation of China (52168010, 41861052), the Basic and Applied Basic Research Project of Guangzhou Basic Research Program (202102020338), the Innovation and Entrepreneurship Training Program for college students of Zhongkai University of Agriculture and Engineering (202011347293), and Guangzhou Social Science Planning Project (2022GZQN18).

**Institutional Review Board Statement:** Not applicable.

**Informed Consent Statement:** Not applicable.

**Data Availability Statement:** Not applicable.

**Conflicts of Interest:** The authors declare that they have no conflict of interest.

## References

1. De Groot, R.S.; Wilson, M.A.; Boumans, R.M. A typology for the classification, description and valuation of ecosystem functions, goods and services. *Ecol. Econ.* **2002**, *41*, 393–408. [\[CrossRef\]](#)
2. Costanza, R. Ecosystem services in theory and practice. *Encycl. Anthr.* **2018**, *3*, 419–422.
3. Small, N.; Munday, M.; Durance, I. The challenge of valuing ecosystem services that have no material benefits. *Glob. Environ. Chang.* **2017**, *44*, 57–67. [\[CrossRef\]](#)
4. Liu, Z.; Wu, R.; Chen, Y.; Fang, C.; Wang, S. Factors of ecosystem service values in a fast-developing region in China: Insights from the joint impacts of human activities and natural conditions. *J. Clean. Prod.* **2021**, *297*, 126588. [\[CrossRef\]](#)
5. Hauck, J.; Görg, C.; Varjopuro, R.; Ratamáki, O.; Maes, J.; Wittmer, H.; Jax, K. “Maps have an air of authority”: Potential benefits and challenges of ecosystem service maps at different levels of decision making. *Ecosyst. Serv.* **2013**, *4*, 25–32. [\[CrossRef\]](#)
6. Costanza, R.; d’Arge, R.; De Groot, R.; Farber, S.; Grasso, M.; Hannon, B.; Limburg, K.; Naeem, S.; Paruelo, J.; Van Den Belt, M.; et al. The value of the world’s ecosystem services and natural capital. *Nature* **1997**, *387*, 253–260. [\[CrossRef\]](#)
7. Li, W.; Wang, L.; Yang, X.; Liang, T.; Zhang, Q.; Liao, X.; White, J.R.; Rinklebe, J. Interactive influences of meteorological and socioeconomic factors on ecosystem service values in a river basin with different geomorphic features. *Sci. Total Environ.* **2022**, *829*, 154595. [\[CrossRef\]](#)
8. Wang, A.; Liao, X.; Tong, Z.; Du, W.; Zhang, J.; Liu, X.; Liu, M. Spatial-temporal dynamic evaluation of the ecosystem service value from the perspective of “production-living-ecological” spaces: A case study in Dongliao River Basin, China. *J. Clean. Prod.* **2022**, *333*, 130218. [\[CrossRef\]](#)
9. Pan, N.; Guan, Q.; Wang, Q.; Sun, Y.; Li, H.; Ma, Y. Spatial differentiation and driving mechanisms in ecosystem service value of arid region: A case study in the middle and lower reaches of Shule River Basin, NW China. *J. Clean. Prod.* **2021**, *319*, 128718. [\[CrossRef\]](#)
10. De Groot, R.; Brander, L.; Van Der Ploeg, S.; Costanza, R.; Bernard, F.; Braat, L.; Christie, M.; Crossman, N.; Ghermandi, A.; van Beukering, P.; et al. Global estimates of the value of ecosystems and their services in monetary units. *Ecosyst. Serv.* **2012**, *1*, 50–61. [\[CrossRef\]](#)
11. Xie, G.; Zhen, L.; Lu, C.; Xiao, Y.; Chen, C. Expert Knowledge Based Valuation Method of Ecosystem Services in China. *J. Nat. Resour.* **2008**, *23*, 911–919.
12. Maimaiti, B.; Chen, S.; Kasimu, A.; Simayi, Z.; Aierken, N. Urban spatial expansion and its impacts on ecosystem service value of typical oasis cities around Tarim Basin, northwest China. *Int. J. Appl. Earth Obs. Geoinf.* **2021**, *104*, 102554. [\[CrossRef\]](#)

13. Song, F.; Su, F.; Mi, C.; Sun, D. Analysis of driving forces on wetland ecosystem services value change: A case in Northeast China. *Sci. Total Environ.* **2021**, *751*, 141778. [[CrossRef](#)]
14. Bernués, A.; Tello-García, E.; Rodríguez-Ortega, T.; Ripoll-Bosch, R.; Casasús, I. Agricultural practices, ecosystem services and sustainability in High Nature Value farmland: Unraveling the perceptions of farmers and nonfarmers. *Land Use Policy* **2016**, *59*, 130–142. [[CrossRef](#)]
15. Ma, X.; Zhu, J.; Zhang, H.; Yan, W.; Zhao, C. Trade-offs and synergies in ecosystem service values of inland lake wetlands in Central Asia under land use/cover change: A case study on Ebinur Lake, China. *Glob. Ecol. Conserv.* **2020**, *24*, e01253. [[CrossRef](#)]
16. Jing, Y.; Chang, Y.; Cheng, X.; Wang, D. Land-use changes and ecosystem services under different scenarios in Nansi Lake Basin, China. *Environ. Monit. Assess.* **2021**, *193*, 21. [[CrossRef](#)]
17. Munang, R.; Thiaw, I.; Alverson, K.; Liu, J.; Han, Z. The role of ecosystem services in climate change adaptation and disaster risk reduction. *Curr. Opin. Environ. Sustain.* **2013**, *5*, 47–52. [[CrossRef](#)]
18. Fang, L.; Wang, L.; Chen, W.; Sun, J.; Cao, Q.; Wang, S.; Wang, L. Identifying the impacts of natural and human factors on ecosystem service in the Yangtze and Yellow River Basins. *J. Clean. Prod.* **2021**, *314*, 127995. [[CrossRef](#)]
19. Chen, M.; Lu, Y.; Ling, L.; Wan, Y.; Luo, Z.; Huang, H. Drivers of changes in ecosystem service values in Ganjiang upstream watershed. *Land Use Policy* **2015**, *47*, 247–252. [[CrossRef](#)]
20. Li, G.; Fang, C.; Wang, S. Exploring spatiotemporal changes in ecosystem-service values and hotspots in China. *Sci. Total Environ.* **2016**, *545*, 609–620. [[CrossRef](#)]
21. Bai, L.; Jiang, L.; Yang, D.Y.; Liu, Y.B. Quantifying the spatial heterogeneity influences of natural and socioeconomic factors and their interactions on air pollution using the geographical detector method: A case study of the Yangtze River Economic Belt, China. *J. Clean. Prod.* **2019**, *232*, 692–704. [[CrossRef](#)]
22. Liu, X.; Wang, H.; Wang, X.; Bai, M.; He, D. Driving factors and their interactions of carabid beetle distribution based on the geographical detector method. *Ecol. Indic.* **2021**, *133*, 108393. [[CrossRef](#)]
23. Wu, C.; Chen, B.; Huang, X.; Wei, Y.D. Effect of land-use change and optimization on the ecosystem service values of Jiangsu province, China. *Ecol. Indic.* **2020**, *117*, 106507. [[CrossRef](#)]
24. Li, X.; Guo, J.; Qi, S. Forestland landscape change induced spatiotemporal dynamics of subtropical urban forest ecosystem services value in forested region of China: A case of Hangzhou city. *Environ. Res.* **2021**, *193*, 110618. [[CrossRef](#)] [[PubMed](#)]
25. Ouyang, X.; Tang, L.; Wei, X.; Li, Y. Spatial interaction between urbanization and ecosystem services in Chinese urban agglomerations. *Land Use Policy* **2021**, *109*, 105587. [[CrossRef](#)]
26. Ghebregabher, M.G.; Yang, T.; Yang, X.; Sereke, T.E. Assessment of NDVI variations in responses to climate change in the Horn of Africa. *Egypt. J. Remote Sens. Space Sci.* **2020**, *23*, 249–261. [[CrossRef](#)]
27. Schindler, K.; Papasaika-Hanusch, H.; Schütz, S.; Baltasavias, E. Improving wide-area DEMs through data fusion-chances and limits. *Proc. Photogramm. Week* **2011**, *11*, 159–170.
28. Redo, D.J.; Aide, T.M.; Clark, M.L.; Andrade-Núñez, M.J. Impacts of internal and external policies on land change in Uruguay, 2001–2009. *Environ. Conserv.* **2012**, *39*, 122–131. [[CrossRef](#)]
29. Hou, L.; Wu, F.; Xie, X. The spatial characteristics and relationships between landscape pattern and ecosystem service value along an urban-rural gradient in Xi'an city, China. *Ecol. Indic.* **2020**, *108*, 105720. [[CrossRef](#)]
30. Dong, M.; Yang, L.; Su, L.; Chang, L.; Gao, D.; Zhou, J. Study on the value and sensitivity of ecosystem services based on land use change: A case study of Daqing City. *J. Saf. Environ.* **2014**, *14*, 330–333.
31. Yue, J.; Xue, L. Study on the dynamics of land use and ecosystem services value in Shanxi Province. *J. China Agric. Univ.* **2020**, *25*, 20–30.
32. Han, R.; Feng, C.C.; Xu, N.; Guo, L. Spatial heterogeneous relationship between ecosystem services and human disturbances: A case study in Chuandong, China. *Sci. Total Environ.* **2020**, *721*, 137818. [[CrossRef](#)] [[PubMed](#)]
33. Getis, A.; Ord, J.K. The analysis of spatial association by use of distance statistics. *Geogr. Anal.* **1992**, *24*, 189–206. [[CrossRef](#)]
34. Su, L.; Ji, X. Spatial-temporal differences and evolution of eco-efficiency in China's forest park. *Urban For. Urban Green.* **2021**, *57*, 12689. [[CrossRef](#)]
35. Wang, J.F.; Zhang, T.L.; Fu, B.J. A measure of spatial stratified heterogeneity. *Ecol. Indic.* **2016**, *67*, 250–256. [[CrossRef](#)]
36. Zhang, N.; Jing, Y.C.; Liu, C.Y.; Li, Y.; Shen, J. A cellular automaton model for grasshopper population dynamics in Inner Mongolia steppe habitats. *Ecol. Model.* **2016**, *329*, 5–17. [[CrossRef](#)]
37. He, J.; Pan, Z.; Liu, D.; Guo, X. Exploring the regional differences of ecosystem health and its driving factors in China. *Sci. Total Environ.* **2019**, *673*, 553–564. [[CrossRef](#)]
38. Yi, H.; Güneralp, B.; Filippi, A.M.; Kreuter, U.P.; Güneralp, İ. Impacts of land change on ecosystem services in the San Antonio River Basin, Texas, from 1984 to 2010. *Ecol. Econ.* **2017**, *135*, 125–135. [[CrossRef](#)]
39. Zhang, Z.; Xia, F.; Yang, D.; Huo, J.; Wang, G.; Chen, H. Spatiotemporal characteristics in ecosystem service value and its interaction with human activities in Xinjiang, China. *Ecol. Indic.* **2020**, *110*, 105826. [[CrossRef](#)]
40. Hu, X.; Hong, W.; Qiu, R.; Hong, T.; Chen, C.; Wu, C. Geographic variations of ecosystem service intensity in Fuzhou City, China. *Sci. Total Environ.* **2015**, *512*, 215–226. [[CrossRef](#)]
41. Ma, L.; Cheng, W.; Bo, J.; Li, X.; Gu, Y. Spatio-temporal variation of land-use intensity from a multi-perspective—Taking the middle and lower reaches of Shule River Basin in China as an example. *Sustainability* **2018**, *10*, 771. [[CrossRef](#)]

42. Jiang, C.; Wang, F.; Zhang, H.; Dong, X. Quantifying changes in multiple ecosystem services during 2000–2012 on the Loess Plateau, China, as a result of climate variability and ecological restoration. *Ecol. Eng.* **2016**, *97*, 258–271. [[CrossRef](#)]
43. Wu, D.; Zou, C.; Cao, W.; Xiao, T.; Gong, G. Ecosystem services changes between 2000 and 2015 in the Loess Plateau, China: A response to ecological restoration. *PLoS ONE* **2019**, *14*, e0209483. [[CrossRef](#)]
44. Song, W.; Deng, X. Land-use/land-cover change and ecosystem service provision in China. *Sci. Total Environ.* **2017**, *576*, 705–719. [[CrossRef](#)] [[PubMed](#)]
45. Zhang, F.; Yushanjiang, A.; Jing, Y. Assessing and predicting changes of the ecosystem service values based on land use/cover change in Ebinur Lake Wetland National Nature Reserve, Xinjiang, China. *Sci. Total Environ.* **2019**, *656*, 1133–1144. [[CrossRef](#)]